中國機械工程學刊第三十九卷第三期第339~344頁(民國一百零七年)
Journal of the Chinese Society ofMechanical Engineers, Vol.39, No.3, pp.339~344(2018)

Study of Hydrogen Combustion in the Off-Gas Burner of Solid Oxide Fuel Cell System

Shing-Cheng Chang*, Tzu-Hsuan Feng**, Yen-Hsin Chan*,**,
Cha'o-Kuang Chen**

Keywords：Solid oxide fuel cell; off-gas burner; Combustion; CFD.

ABSTRACT

The afterburner is an important components for thermal balance in a solid oxide fuel cell system. The chemical energy of the off-gases from anode and cathode is changed to heat energy for thermal balance of system and further heat recovery and reuse. This study uses the computational fluid dynamics to simulate the combustion flow field in the afterburner. The flue gas is mixed by hydrogen and nitrogen carrying gases at different ratio. The effects of afterburner geometric size is also studied in this researches. The results show that the amount of nitrogen gases significantly affects the thermal uniformity and outlet temperature. In the study cases, the temperature of exhaust gases is reduced to be less than 950°C as the hydrogen components is less than 60% of the mixing fuel gas. In the case, the system cost can be reduced by using common materials which cannot be operated at high temperature above 1000°C.

INTRODUCTION

With the increasing demand for energy, the development of sustainable, low-pollution and high-efficiency alternative energy technologies has become the most important issue in the world. Recently, the fuel cells which convert the chemical energy of hydrogen-containing fuel gas into electrical energy are considered one of the most promising technologies for green energy. By the protons produced in anode or oxygen ions produced in cathode passing through the electrolytes to another electrode, the fuel cells generate power at appropriate production.

Among various types of fuel cells, the solid oxide fuel cell (SOFC) (Choudhury et al., 2013) operates at a high temperature of 800-1000°C with a relative high efficiency up to 60%. Even in an intermediate SOFC, it also requires 550-700°C to achieve a good oxygen ion conductivity (Brett et al., 2008; Cheng et al., 2016). As a result, hydrocarbon fuel gases like methane are also adoptable for SOFCs to generate power through the internal reformation of fuel gases to hydrogen, i.e. the fuel sources of SOFCs are diverse.

Generally, the fuel utilization of SOFCs is above 70%, and the remaining fuel gases are introduced into an afterburner to convert chemical energy into heat energy by combustion. Then the heat energy is used for the fuel and air pre-heating of the system by using heat exchanger, and also used for hot air or water production to further improve the system efficiency up to 90% (Onda et al., 2003; Braun et al., 2006). Another solution for residual hydrogen gas is fuel reuse. For example, Somekawa et al. (2017) presented a two-stage SOFC stack configuration, in which the remaining fuel that are not used at the 1st SOFC stack are introduced into the 2nd stack. The total fuel utilization of the system is 92% and the electrical efficiency is 77.8% (DC, LHV). However, to remove the H_2O and CO_2 in the fuel exiting 1st SOFC, an off-gas regenerating technique was used accompanied with the 2nd stack and hence increased the system cost. Therefore, the cost down issue of this scheme is important in the progressive development.

Since the temperature of SOFC off-gases usually exceed the self- ignition temperature of hydrogen, the gas combustion in a SOFC afterburner is high efficiency. The heat recovery of high-temperature exhaust gas is implemented through the heat exchanger to preheat air and provide the heat energy required for fuel reformer. As one of the most important key components of the SOFC system, the afterburner must be able to convert low-calorific value gases into thermal energy during system operation. When the system is shut down, the afterburner must convert the high-heat reformate gas.

Frenzel et al (2011) listed components of anode off-gas corresponding to the operation of the SOFC, as

Paper Received June, 2018. Revised June, 2018. Accepted June, 2018.Author for Correspondence: Cha'o-Kuang Chen.

**Green Energy & Environment Research Laboratories, Industrial Technology Research Institute, Tainan, Taiwan., ROC.*

*** Department of Mechanical Engineering, National Cheng Kung University, Tainan, Taiwan, ROC.*

well as the components at system startup and shutdown. The gases mainly include H_2, CO, CO_2, N_2, H_2O. At different power generation and fuel utilization rates, the proportion of gas composition is also different. Therefore, for the power generation and component configuration of the SOFC system, the afterburner design needs to meet the performance requirements.

In terms of structural design, Hong et al. (2013) presented a 2kW SOFC system. An afterburner without fuel and air premixing was used to avoid high-temperature flash over of the fuel. The operational control is relatively easy in this case. Frenzel et al. (2011) proposed a burner with a two-stage combustion mechanism. As the system is operating, the fuel off-gas can be completely combusted in the first combustion chamber with high temperature air diverted into the reactor. When the system is turned on/off, the high-heat-value reformed gas that has not been burned in the first combustion chamber enters the second combustion chamber with the combustion exhaust gas and reacts with more high-temperature air. Through the action of this two-stage combustion gas, the energy of the unreacted fuel gas entering the SOFC can be completely converted into heat energy for further recycling.

Pianko-Oprych and Jaworski (2017) used computational fluid dynamics simulation (CFD) to study the performance of an afterburner proposed by Sunfire. The inlet flow channels for SOFC anode exhaust gas and natural gas are different. The combustion chamber is divided into two parts, i.e. the startburner and afterburner. The simulation results were consistent with the experimental data. It shows that the numerical simulation is suitable for the characteristic research and technical development of the SOFC burner.

Since the literatures and reports of the SOFC afterburner are few, it is necessary to study the characteristic of the afterburner for SOFC system operation. This study uses the CFD to simulate the combustion of the SOFC afterburner. To simply the exhaust gas components, pure hydrogen gas is used in this work combined with nitrogen carrying gas. The characteristics of flow field in the afterburner are investigated as the hydrogen/ nitrogen ratio is changed.

METHODOLOGY

Governing equations

The conservation equations are solved in the numerical simulations of the SOFC afterburner including:

(1) Continuity equation

$$\frac{\partial \rho}{\partial t}+\frac{\partial}{\partial x_i}(\rho u_i)=0 \tag{1}$$

where ρ, t and u_i are the fluid density, evolution time, and flow velocity at i direction respectively.

(2) Reynolds-averaged Navier–Stokes equations (RANS)

$$\frac{\partial \rho}{\partial t}(\rho u_i)+\frac{\partial \rho}{\partial x_j}(\rho u_i u_j) =-\frac{\partial P}{\partial x_i}+\frac{\partial}{\partial x_j}\left[\mu\left(\frac{\partial u_i}{\partial x_j}+\frac{\partial u_j}{\partial x_i}-\frac{2}{3}\delta_{ij}\frac{\partial u_l}{\partial x_l}\right)\right] +\frac{\partial}{\partial x_j}\left(-\rho\overline{u_i' u_j'}\right) \tag{2}$$

where p is pressure, μ is fluid viscosity, and $\overline{u_i' u_j'}$ is the terms of Reynolds stress.

(3) The standard k-ε turbulence model

$$\frac{\partial}{\partial t}(\rho k)+\frac{\partial}{\partial x_i}(\rho k u_i) =\frac{\partial}{\partial x_j}\left[\left(\mu+\frac{\mu_t}{\sigma_k}\right)\frac{\partial k}{\partial x_j}\right]+G_k+G_b+-\rho\varepsilon-Y_M+S_k \tag{3}$$

$$\frac{\partial}{\partial t}(\rho\varepsilon)+\frac{\partial}{\partial x_i}(\rho\varepsilon u_i) =\frac{\partial}{\partial x_j}\left[\left(\mu+\frac{\mu_t}{\sigma_\varepsilon}\right)\frac{\partial \varepsilon}{\partial x_j}\right]+C_{1\varepsilon}\frac{\varepsilon}{k}(G_k+C_{3\varepsilon}G_b) -C_{2\varepsilon}\rho\frac{\varepsilon^2}{k}+S_\varepsilon \tag{4}$$

In the equations, G_k is the turbulent kinetic energy generation term due to the average velocity gradient, and G_b is the turbulent kinetic energy generation term due to buoyancy. The term Y_M represents the contribution of the expansion expansion to the overall dissipation rate in the compressible turbulent flow, and μ_t is the turbulent flow viscosity. The coefficients, σ_k and σ_ε, are the turbulent Prandtl number of k and ε.

(4) The energy equations

$$\frac{\partial}{\partial t}(\rho E)+\frac{\partial}{\partial x_i}[u_i(\rho E+p)] =\frac{\partial}{\partial x_j}\left[\left(k+\frac{c_p\mu_t}{Pr_t}\right)\frac{\partial T}{\partial x_j}+u_i(\tau_{ij})_{eff}\right]+S_h \tag{5}$$

where E is the total energy, c_p is the heat capacity under constant pressure, T is the temperature, and S_h is the heat source. $(\tau_{ij})_{eff}$ is the deflection stress tensor defined as

$$(\tau_{ij})_{eff}=\mu_{eff}\left(\frac{\partial u_i}{\partial x_j}+\frac{\partial u_j}{\partial x_i}\right)-\frac{2}{3}\mu_{eff}\frac{\partial u_i}{\partial x_i}\delta_{ij} \tag{6}$$

(5) The Chemical species transmission equation

As the Species Transport model is used to calculate the chemical reaction part, the Y_i solution equation for each chemical species needs to be expressed as

$$\frac{\partial}{\partial t}(\rho Y_i)+\frac{\partial}{\partial x_j}(\rho u_j Y_i)=-\frac{\partial J_{ij}}{\partial x_j}+R_i+S_i \tag{7}$$

where J_{ij} is the diffusive flux of type i, R_i is the net generation rate of i type due to chemical reaction, and S_i is the source term.

(6) Mixture fraction transmission equation

The mixture fraction is defined as

$$f=\frac{Z_i-Z_{i,ox}}{Z_{i,fuel}-Z_{i,ox}} \tag{8}$$

Where Z_i is the mass fraction of the element i. the subscript ox represents the value at the oxidant inlet, and the subscript fuel represents the value at the fuel inlet. The Favre average (density average) mixture fraction formula is

$$\frac{\partial}{\partial t}(\rho\bar{f})+\frac{\partial}{\partial x_i}(\rho u_i\bar{f}) = \frac{\partial}{\partial x_j}\left[\left(\frac{k}{C_p}+\frac{\mu_t}{\sigma_t}\right)\frac{\partial\bar{f}}{\partial x_j}\right]+S_m \tag{9}$$

where k is the laminar heat transfer coefficient of the mixture, C_p is the specific heat of mixing, σ_t is the Prandtl number, and S_m is the source term. The mixture fraction variation $\overline{f'^2}$ can be obtained by

$$\frac{\partial}{\partial t}\left(\rho\overline{f'^2}\right)+\frac{\partial}{\partial x_i}\left(\rho u_i\overline{f'^2}\right) = \frac{\partial}{\partial x_j}\left[\left(\frac{k}{C_p}+\frac{\mu_t}{\sigma_t}\right)\frac{\partial\overline{f'^2}}{\partial x_j}\right]+C_g\mu_t\left(\frac{\partial\bar{f}}{\partial x_j}\right)^2-C_d\rho\frac{\varepsilon}{k}\overline{f'^2} \tag{10}$$

where $f' = f-\bar{f}$.

Simulation model

The simulation model in this study is shown in Figure 1 and the mathematical model used in this study is listed in Table 1. The flow rate of off-gases is set for high power generation SOFC. The boundary conditions are as follows:

Air inlet: $\dot{Q} = \dot{Q}_{air}$ L/min，$T = 973\ K$

Fuel inlet: $\dot{Q} = \dot{Q}_{fuel}$ L/min，$T = 1073\ K$

Outlet: $P = P_\infty = 101.325$ kPa

Inner walls: no-slip and no-penetration conditions

Outer inner walls: adiabatic

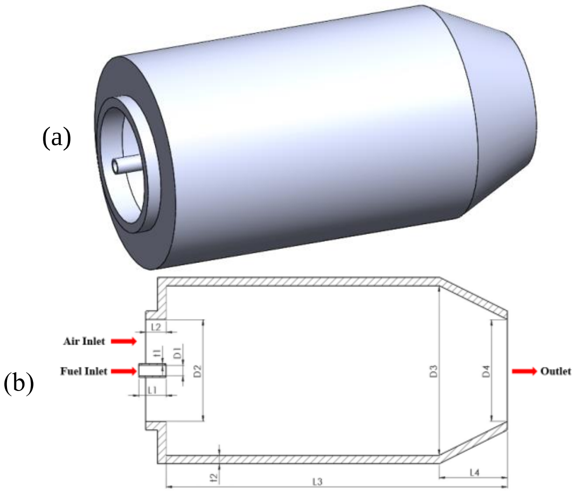

Fig. 1.Simulation model of SOFC afterburner.

Table 1.The mathematical model of simulation.

Calculation Conditions	**Selected Model**
Space	Three Dimensional
Time	Steady
Material	Fluid：Gas mixture Solid：Al_2O_3
Equation of State	Ideal Gas
Viscous Regime	Turbulent
Reynolds-Average Turbulence	Standard $k-\varepsilon$ Turbulence
Reacting Flow	Species Transport、 Non-Premixed Combustion
Radiation	P1

Table 2. Geometric parameters and gas flow rates (in mm, L/min)

Case	L_1	L_2	L_3	L_4	D_1	D_2	D_3	D_4	t_1	t_2	$\dot{Q}_{air}$	$\dot{Q}_{fuel}$
1	100	60	1000	200	50	200	300	200	5	25	750	500
2	100	60	1000	200	50	300	500	300	5	25	750	500
3	100	60	1000	200	30	300	500	300	5	25	750	500

RESULTS AND DISCUSSIONS

The numerical verification is achieved by simulating the non-premixed turbulent flame of hydrogen/air downstream co-current injector with comparison to Alliche and Chikh’s results (2018). In the case, the conjugate heat transfer is ignored with adiabatic wall boundary. In this study, the Al_2O_3 thermal insulation walls are applied in the simulation of afterburner.

Combustion of pure hydrogen

The combustion of pure hydrogen is simulated in the first parts of the present work. The geometric parameters and gas flow rates are listed in Table 2 to study the effects of burner geometric sizes. Figure 2(a) presents the temperature distribution of combustion chamber in the case 1. Because the fuel gas and air are parallel flow, the hydrogen molecules with small radial velocity are difficultly diffused into air to produce combustion flame. Consequently, the combustion reaction starts from the outside of the hydrogen column and causes a long flame. The maximum temperature of the chamber is 2360K and the wall temperature is between 1070 K and 1100 K. Because the flame is wider, the outlet temperature of 2184 K is higher than the front of the combustion chamber. Figure 2(b) shows that there are residual hydrogen gas at the outlet. Therefore, the length of the combustion chamber should be extended in order to avoid high-temperature exhaust hydrogen gas.

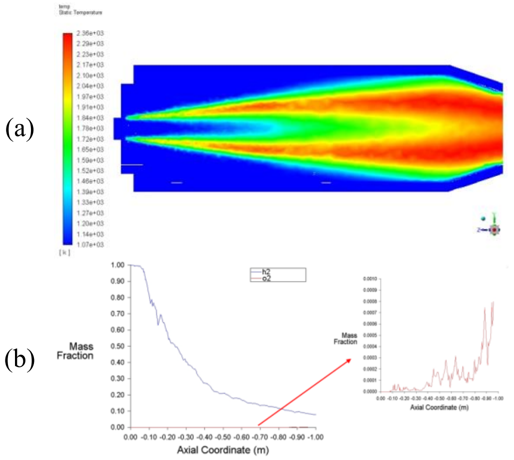

Fig. 2.(a) Temperature distribution and (b) mass fraction of hydrogen and oxygen on the central axis in case 1.

In case 2, the temperature in the chamber is less than that of case 1 due to an increase chamber size (outlet temperature: 2110 K; wall temperature: between 1070 K and 1080 K). When the fuel inlet size is reduced, as in case 3, the gas mixing is enhanced and the amount of residual hydrogen gas at outlet is decreased. The simulation results of case 3 are shown in figure 4. As a result of hydrogen combustion improving, the average outlet temperature is increased to 2449 K, and the wall temperature is between 955 K and 1010 K, which is lower than that of Case.2 and Case.3.

From above case studies, it can be found that the fuel inlet pipe diameter has a significant effect on the flame length and outlet temperature. Therefore, when designing the combustion chamber, diameters of fuel inlet pipes must be selected for specific cases. The length of combustion chamber is also adjusted for completely combustion for hydrogen gas. In this cases, the pressure drop is very small (2~12 Pa).

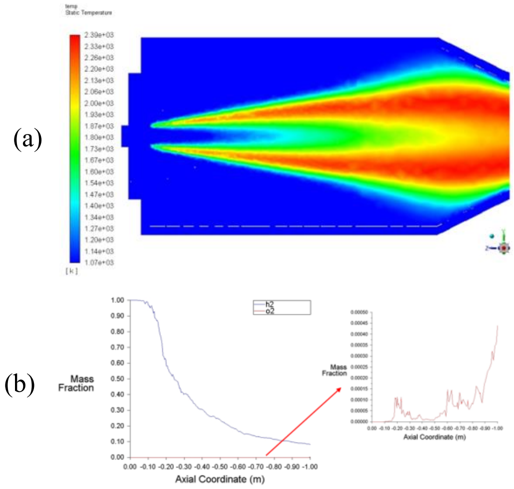

Fig. 3.(a) Temperature distribution and (b) mass fraction of hydrogen and oxygen on the central axis in case 2.

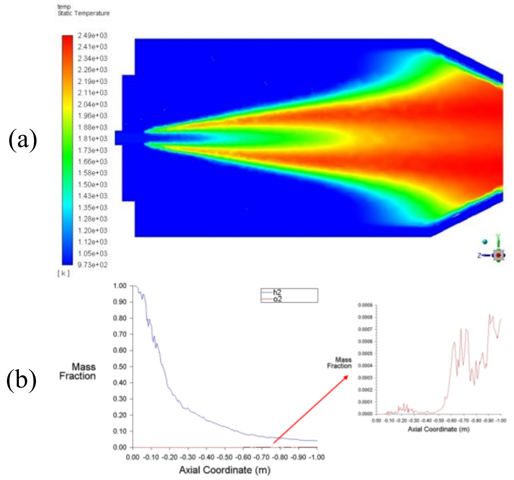

Fig. 4.(a) Temperature distribution and (b) mass fraction of hydrogen and oxygen on the central axis in case 3.

Combustion of hydrogen/nitrogen mixing gases

In this section, the combustion characteristics of hydrogen/nitrogen mixing gases is investigated for the SOFCs which need additional carrying gas at anode. Five cases of ratio at 100%, 80%, 60%, 40% and 20% are simulated. The hydrogen flow required is 500 L/min, and the ratio of fuel to oxidant is fixed at 1:1.5. The geometries of these cases are the same as the case 3 in Table 2, i.e. case 3 is the case of H_2- 100%@N_2.

Table 3. The inlet flow rate under various hydrogen/nitrogen ratio.

Ratio ($\frac{\dot{Q}_{H_2}}{\dot{Q}_{H_2}+\dot{Q}_{N_2}}$)	Fuel		Oxidizer
	$\dot{Q}_{H_2}$ (L/min)	$\dot{Q}_{N_2}$ (L/min)	$\dot{Q}_{Air}$ (L/min)
100%	500	0	750
80%	500	125	937.5
60%	500	333	1249.5
40%	500	750	1875
20%	500	2000	3750

Figure 5 shows the results of H_2- 80%@N_2. By comparing with Fig. 3, the average exit temperature is reduced to 2315 K, while the wall temperature ranged from 970 K to 1010 K is not changed. Figure 5(b) shows the amount of residual hydrogen gas is reduced, but not equao to zero at the exit of burner. As the hydrogen/nitrigen ratio decreases to 60%, the combustion temperaure of the chamber is significantly reduced due to the large amount of introducing nitrigen gas and air. The wall temperature is about 970-1000K acompanying with the exit temperature of 1028K, as shown in Fig. 6. The flame shape is shortened as well.

In the cases of hydrogen/nitrigen ratio at 40% and 20%, the exit temperature is less than 750K, and the wall temperature ranges in 820K to 980K. As shown in Figs. 7 and 8, the uniformity of chamber temperature is improved. Due to the narrow fuel inlet,

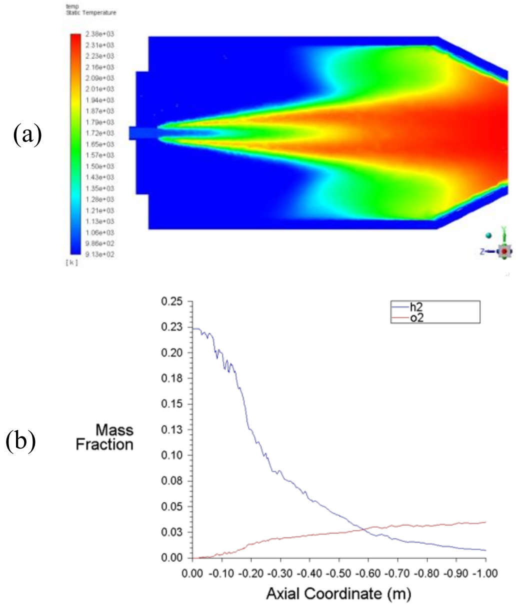

Fig. 5. (a) Temperature distribution and (b) mass fraction of hydrogen and oxygen on the central axis in the case of H2- 80%@N2.

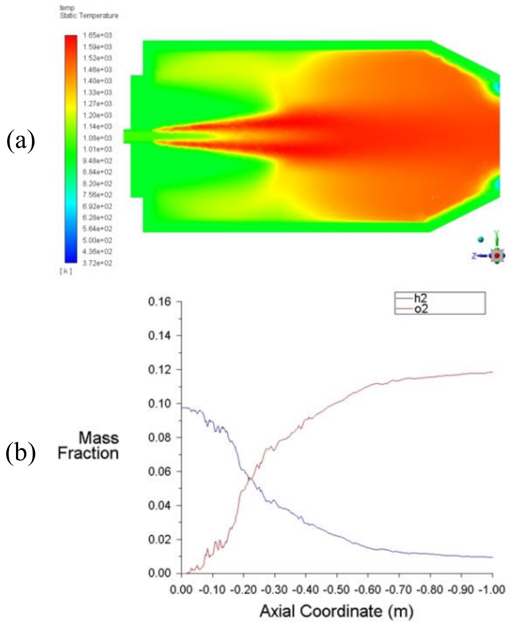

Fig. 6. (a) Temperature distribution and (b) mass fraction of hydrogen and oxygen on the central axis in the case of H2- 60%@N2.

increasing the nitrigen amount of the mixing gases would enlarge the flame velocity, and hence narrow the flame width. As in Fig. 7, an injecting flame is observed.

CONCLUSIONS

This study conducted the CFD simulation model for the SOFC afterburner. The flow field and combustion phenomena inside the afterburner chamber were analyzed. The results of various

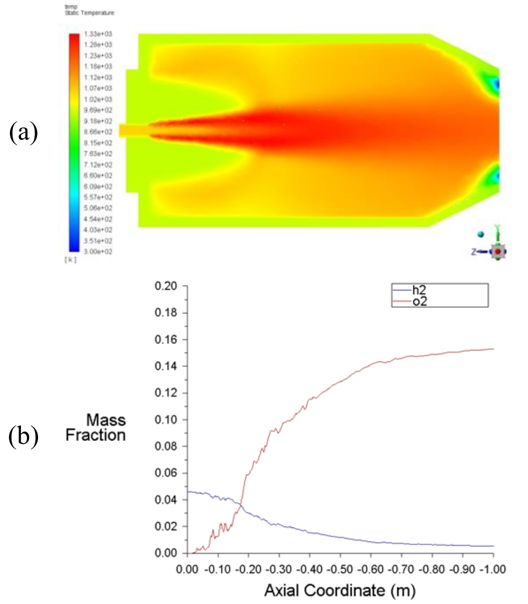

Fig. 7. (a) Temperature distribution and (b) mass fraction of hydrogen and oxygen on the central axis in the case of H2- 40%@N2.

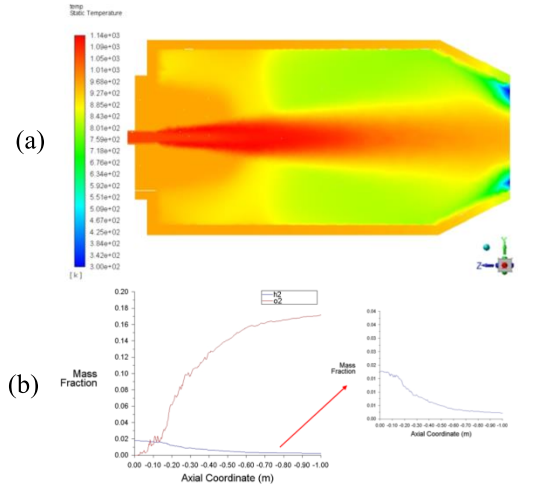

Fig. 8. (a) Temperature distribution and (b) mass fraction of hydrogen and oxygen on the central axis in the case of H2- 20%@N2.

hydrogen/nitrogen ratio show that the temperature of exhaust gases can be reduced to < 950°C, which is a common index for afterburner for SOFC system costdown, as the hydrogen components is less than 60% of the mixing fuel gas. Reducing the chamber operating temperature also mean the afterburner size can be decreased. Besides, the increase of air amount leads to oxygen-enriched combustion, which is helpful for complete combustion of large hydrogen flow rate, as in this study. Generally, the hydrogen-nitrogen ratio of fuel gases has significant effects on the combustion characteristics of an afterburner and can be modulated for specific SOFC system.

ACKNOWLEDGEMENT

We gratefully appreciate the financial support from the Bureau of Energy (BOE), Ministry of Economy Affair (MOEA), Taiwan (107-D0901).

REFERENCES

Braun, R. J., Klein, S. A. and Reindl, D. T., “Evaluation of system configurations for solid oxide fuel cell-based micro-combined heat and power generators in residential applications,” Journal of Power Sources, Vol. 158, 1290－1305, 2006.

Brett, D. J., Atkinson, A., Brandon, N. P., and Skinnerd, S. J., “Intermediate temperature solid oxide fuel cells,” Chemical Society Review, Vol.37, 1568–1578, 2008.

Cheng, T. C., Huang, T. Y., Chen, C. F., Tseng, C. J., Lee, S. W., Chang, J. K. and Jang, J., “Analysis of an intermediate-temperature proton conducting SOFC hybrid system,” International Journal of Green Energy, Vol. 13, 1640–1647, 2016.

Choudhury, A., Chandra, H., and Arora, A., “Application of solid oxide fuel cell technology for power generation—A review,” Renewable and Sustainable Energy Reviews, 20, pp. 430–442, 2013.

Frenzel, I., Loukou, A., Trimis, D., An innovative burner concept for the conversion of anode off-gases from high temperature fuel cell systems, 11th Conference on Energy for a Clean Environment 5-8, July 2011.

Mounir Alliche, Salah Chikh. Study of non-premixed turbulent flame of Hydrogen/air downstream Co-Current injector. International journal of hydrogen energy 43, 3577-3585, 2018.

Onda, K., Iwanari, T., Miyauchi, N., Ito, K., Ohba, T., Sakaki, Y. and Nagata, S., “Cycle Analysis of Combined Power Generation by Planar SOFC and Gas Turbine Considering Cell Temperature and Current Density Distributions,” Journal of the Electrochemical Society, Vol. 150, A1569-A1576, 2003.

Pianko-Oprych, P., Jaworski, Z., Numerical investigation of a novel burner to combust anode exhaust gases of SOFC stacks, Polish Journal of Chemical Technology, 19, 20-26, 2017.

Somekawa, T., Nakamura, K., Kushi, T., Kume, T., Fujita, K., and Yakabe, H., “Examination of a high-efficiency solid oxide fuel cell system that reuses exhaust gas,” Applied Thermal Engineering, 114, pp. 1387–1392, 2017.

Wen-Tang Hong, Tzu-Hsiang Yen, Cheng-Nan Huang, Hsueh-I Tan, Yu Chao, Design and development of major balance of plant components in solid oxide fuel cell system, International Journal of Energy and Environment, 4, pp.73-84, 2013.

固態氧化物燃料電池尾氣燃燒器的氫燃燒研究

張勳承
工業技術研究院綠能與環境研究所

馮子軒
國立成功大學機械工程學系

詹彥信
工業技術研究院綠能與環境研究所
國立成功大學機械工程學系

陳朝光
國立成功大學機械工程學系

摘要

尾氣燃燒器是固體氧化物燃料電池系統自主熱平衡所需之的重要熱組件，來自陽極和陰極的廢氣的化學能量轉化為熱能後，進一步回收熱量和再利用。本研究建構計算流體力學模型來研究尾氣燃燒器內部，燃料氣體由氫氣和氮氣以不同比例進行混合。本論文亦分析尾氣燃燒器幾何尺寸對燃燒特性之影響。計算模擬研究結果顯示，燃料氣體之氫/氮比多寡，對後燃器中熱均匀性和出口溫度均有顯著的影響。在本論文的研究案例中，當氫氣成分低於混合燃料氣體的 60%，排氣溫度可降低到低於 950℃。此溫度為一般 SOFC 尾氣燃燒器的設計規格，可減少系統運轉時所需的耐高溫管閥件使用量，進而降低系統建置成本。